Journal of Wood Science

NOTE

Open Access

Porosity analysis of three types of balsa (*Ochroma pyramidale*) wood depending on density

Eun-Suk Jang and Chun-Won Kang*

Abstract

Balsa (*Ochroma pyramidale*), which is the lowest density wood, is a useful species in various industries. In general, balsa can be divided into three types (low density: LD, middle density: MD, high density: HD). In this study, we classified the porosities of the three balsa types into through-pore porosity, blind-pore porosity, and closed-pore porosity. As a result, the total porosity of balsa showed a high positive (+) correlation with closed-pore porosity, but total porosity of balsa showed negative (−) correlations with blind-pore porosity and through-pore porosity. Such information can be useful when using balsa as a natural porous material.

Keywords: Balsa, *Ochroma pyramidale*, Through-pore porosity, Blind-pore porosity, Closed-pore porosity

Introduction

Balsa (*Ochroma pyramidale*), a typical low-density wood, is used widely in industrial applications that require lightweight materials such as thermal insulation, wind turbine blades, and manufacturing of aircraft [1, 2]. Moreover, balsa is the preferred material for high-rise sandwich panels [3, 4].

When balsa is used as a core material, its elastic properties are very important. From a prior study, the axial compressive Young's modulus and strength of balsa tend to increase linearly depending on density. In other words, the mechanical capability of balsa is dependent on its density [4–6].

Balsa's density range is wide, from approximately 0.06 to 0.38 g cm^{-1}. Typically, balsa can be separated based on density: low density (LD) less than 0.1 g cm^{-1}, middle density (MD) of 0.1–0.2 g cm^{-1}, and high density (HD) greater than 0.2 g cm^{-1} [3]. Normally, wood density is constant, and the lower is the density of the wood, the higher is its porosity [7].

The pore analysis of wood is critical as a basis for studying the macro-physical properties of wood [8]. Methods for analyzing wood's pore structure include an anatomical method using a microscope and physical methods using fluid or gas [8, 9].

Borrega et al. [10] analyzed the anatomical features of LD (0.064 g cm^{-1}), MD (0.163 g cm^{-1}), and HD (0.274 g cm^{-1}) balsa by electron microscopy. The lengths of the major axes of the vessels were approximately 220.4 for LD, 320.8 for MD, and 258.8 μm for HD, respectively, and the lengths of the minor axes were approximately 156.6 for LD, 251.0 for MD, and 206.6 μm for HD, respectively. In addition, balsa's fiber volume fraction was 76.3 for LD, 73.5 for MD, and 66.4 for HD. Pan et al. [11] analyzed the pore structure of balsa wood by mercury intrusion porometry and reported that the pore size was 0.1–100 μm, with porosity of approximately 89.5%.

However, few previous studies have analyzed pore structure of the three types of balsa (LD, MD, and HD) using physical methods. Therefore, we focused on the analysis of pore structure of three types of balsa using a physical method.

*Correspondence: kcwon@jbnu.ac.kr

Department of Housing Environmental Design, and Research Institute of Human Ecology, College of Human Ecology, Jeonbuk National University, Jeonju 54896, South Korea

According to the International Union of Pure and Applied Chemistry (IUPAC) [12], pores are classified as through pores when both ends are connected to the external environment, as blind pores when only one side is connected to the outside, or as closed pores when there is no external connection.

Wood is an anisotropic material with different anatomical characteristics depending on the cut direction [13]. The surfaces of tangential and radial planes are almost non-porous; however, the surface of the transverse plane displays a pore structure. Thus, permeability of the transverse section is much higher than that in the other two directions [14]. However, most timber industries use tangential and radial planes. From the point of view of porosity, when wood is used in the tangential and radial planes, the pore structure of the wood is closed. Unlike other wood species, balsa is used in the transverse plane in sandwich panels. Therefore, classification of porosity is important for understanding balsa's porous properties.

Thus, in this study, the pore structure of the balsa transverse section was investigated. Accordingly, three types of balsa were prepared according to density, and porosity analysis (through pore, blind pore, and closed pore) was performed. It is expected that this study will be of great utility to wood researchers.

Materials and methods

Specimen preparation

Figure 1 depicts the preparation of specimens in this study. Three types of North American Balsa (*Ochroma pyramidale*) logs were prepared. Their densities were 0.13 ± 0.03 ($\pm$ standard deviation) for LD, 0.22 ± 0.01 for MD, and 0.39 ± 0.01 g cm^{-3} for HD. The logs were milled into 29-mm-diameter rods and cut into 10-mm-thick cylindrical specimens with a table saw. In order to conduct porosity analysis, 13 specimens for each type were selected. In addition, for morphology analysis, one specimen of each type was selected. It was confirmed by visual inspection that none of the specimens contained knots. Balsa logs were supplied from the Woodworker's Emporium (Las Vegas, NV, USA). Specimen production was carried out in Saehan Timber Co., Ltd. (Gyeonggi-do, Ilsan, Korea). We kept the samples in a standard laboratory environment at 20 °C and 50% humidity for 2 weeks. The moisture content (MC) of the specimens was 6.67% for LD, 6.94% for MD, and 7.38% for HD.

Morphological analysis by SEM (scanning electron microscopy)

The transverse planes of the three types of balsa were observed with SEM (model: Genesis-1000, Emcrafts, Korea) at 100× magnification for vessels and 10,000× magnification for cell walls. The specimen

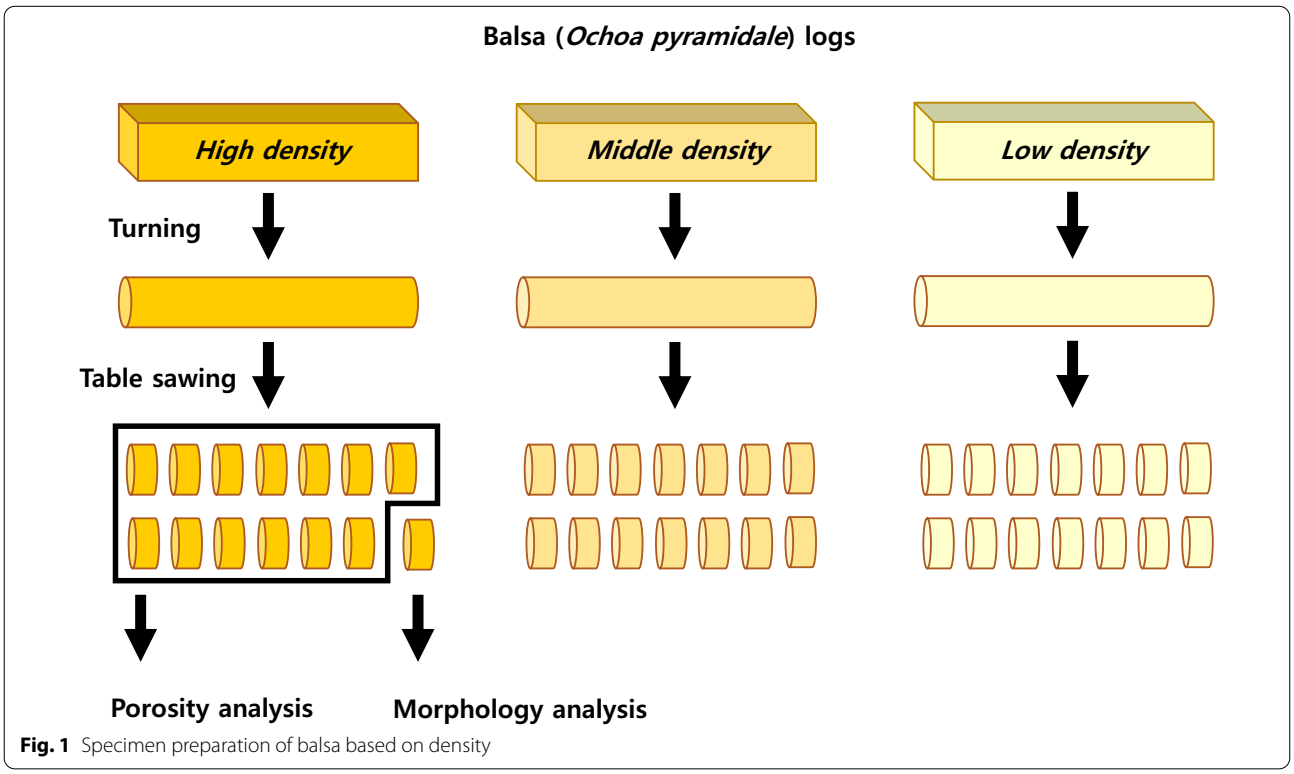

Fig. 1 Specimen preparation of balsa based on density

pretreatment process was as follows: Specimens were cut to a size of about 5 (W) × 5 (D) × 5 (H) mm cube. They were immersed in 10% ethanol and decompressed to –0.1 MPa in a vacuum chamber for 30 min. Next, the surface was shaved by a microtome, and the cube specimens were dried in an oven at 40 °C for 5 h. Finally, they were coated with gold ions. We measured vessel diameter, vessel area, and cell wall thickness using an image software (model: Virtuoso ver 1.1, Emcraft, Korea).

Pore size measurement

We measured the pore sizes of three types of balsa using a capillary flow porometer (model: CFP-1200AEL, PMI Inc, Ithaca, NY, USA) based on the bubble point method of ASTM F-316 [15]. The specimens were immersed in wetting liquid (model: Galwick, PMI Inc, Ithaca, NY, USA), and air pressure was applied to each. The initial pressure at which the wetting liquid was extruded from the specimen was detected. The pore size is calculated as in Eq. 1:

$$D = \frac{C\tau}{p} \tag{1}$$

where D = pore size (μm), τ = surface tension of wetting liquid (dyne cm^{-1}), p = pressure (psi), and C = constant (0.415).

Porosity classification

Porosity refers to the pore volume ratio of a porous material. Therefore, the total porosity (ϕ_{total}) of a cylindrical specimen is defined by Eq. 2:

$$\phi_{total} = \left(1 - \frac{\rho}{\rho_{true}}\right) \times 100 \tag{2}$$

where, for convenience, ρ = density of the cylindrical specimen, and ρ_{true} = true density of the wood (assumed to be 1.5 g cm^{-3}) [7].

The closed-pore porosity (ϕ_{closed}) and open-pore porosity (ϕ_{open}) of the cylindrical specimen can be measured with a gas pycnometer (PYC-100A-1, Porous Materials Inc. USA) [16]. Open-pore porosity is the sum of blind-pore porosity (ϕ_{blind}) and through-pore porosity ($\phi_{through}$) (Eq. 3):

$$\phi_{open} = \phi_{blind} + \phi_{through} \tag{3}$$

In our previous work, we proposed a method to distinguish between blind and through pores [17–20]. We followed the same procedure in this study. First, the cylindrical specimen was wetted in Galwick solution (Porous Materials Inc. USA), which is assumed to penetrate the open pores. Galwick solution has a low surface tension (15.9 dyne cm^{-1}) and is absorbed very quickly. Next, the cylindrical specimen was placed in a hollow-bottom chamber, and air pressure was applied longitudinally. It was assumed that only Galwick solution in the through pores of the cylindrical specimen was extruded. Finally, the cylindrical specimen was weighed. The blind-pore volume (V_{blind}) of the cylindrical specimen was obtained by calculating the difference in cylindrical specimen weight before and after wetting with Galwick solution (Eq. 4):

$$V_{blind} = \frac{m_1 - m_0}{\rho_{Galwick}} \tag{4}$$

where m_0 = specimen weight (g), m_1 = specimen weight after Galwick solution extruded (g), and $\rho_{Galwick}$ = density of Galwick solution (1.79 g cm^{-3}).

The blind-pore porosity of a cylindrical specimen can be calculated by Eq. 5:

$$\phi_{blind} = \frac{V_{blind}}{V_{total}} \times 100 \tag{5}$$

where V_{total} = specimen volume (cm^3).

The through-pore porosity of a cylindrical specimen can be calculated by Eq. 6:

$$\phi_{through} = \phi_{open} - \phi_{blind} \tag{6}$$

In addition, we performed a one-way analysis of variance (ANOVA), and Duncan's multiple range tests determined the significance of the difference at a 10% level ($p < 0.1$).

Results and discussion

SEM images of balsa depending on density

Figure 2 shows SEM images of the balsa transverse plane depending on specimen density, while Table 1 provides vessel diameter, vessel area, and cell wall thickness in three types of balsa wood.

Their vessel arrangement was in the shape of diffuse-porous wood. As for the major axis of the vessel, LD and MD were larger than HD. In minor axis, MD was larger than LD and HD. The vessel area also showed that MD was larger than LD and HD. The cell wall thickness was thinner in LD than in MD and HD.

Results of pore size and porosity analysis

Figure 3a shows the pore sizes of the three types of balsa. The pore size of LD was 148.57 ± 13.47^{c}, 138.69 ± 12.27^{b} for MD, and 117.33 ± 3.98^{a} μm for HD. As a result, pore size of the HD is higher in all three types of balsa (different letters denote significant differences between groups at a 10% level).

Figure 3b shows the three types of balsa's porosity analysis. The total porosity of the balsa calculated from

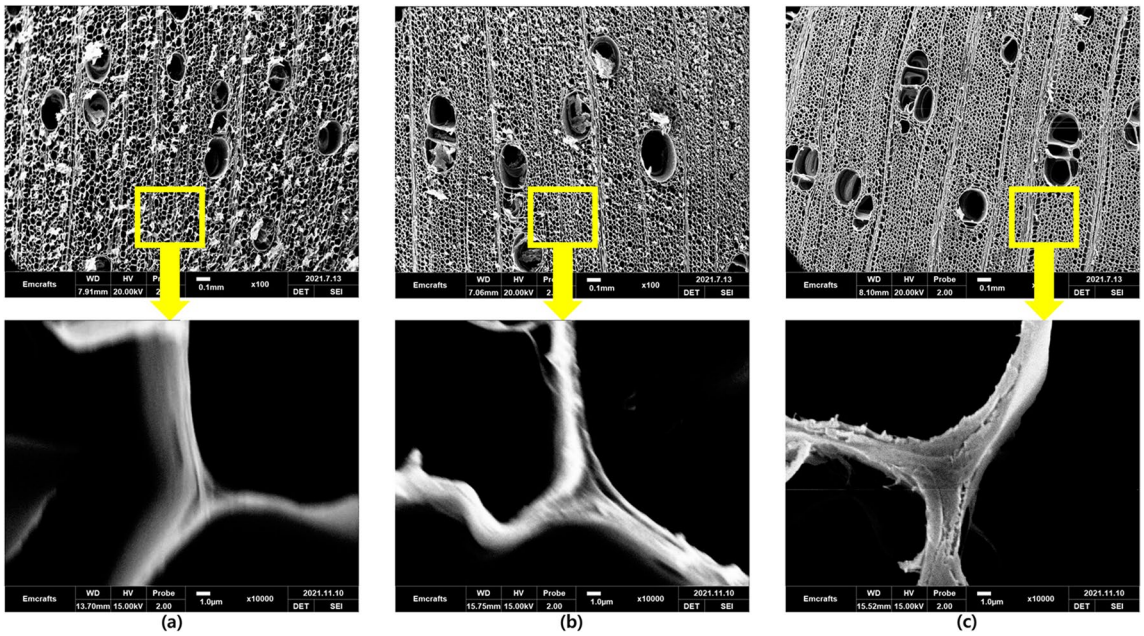

Fig. 2 SEM images of balsa depending on density: **a** LD, **b** MD, **c** HD

Table 1 Results of vessel diameter, vessel area, and cell wall thickness in three types of balsa wood

Balsa wood	Vessel diameter (μm)		Vessel area ($μm^3$)	Cell wall thickness (μm)
	Major axes	Minor axes		
LD	232.80 ± 33.73[b]	148.30 ± 25.49[a]	28,469.10 ± 8186.17[a]	1.52 ± 0.23[a]
HD	243.56 ± 86.82[b]	196.44 ± 24.43[b]	43,931.67 ± 15,505.94[b]	2.13 ± 0.10[b]
MD	169.15 ± 42.74[a]	144.25 ± 49.14[a]	27,322.54 ± 10,244.22[a]	2.48 ± 0.24[b]

± is standard deviation

Different letters denote significant differences between groups at a 10% significance level

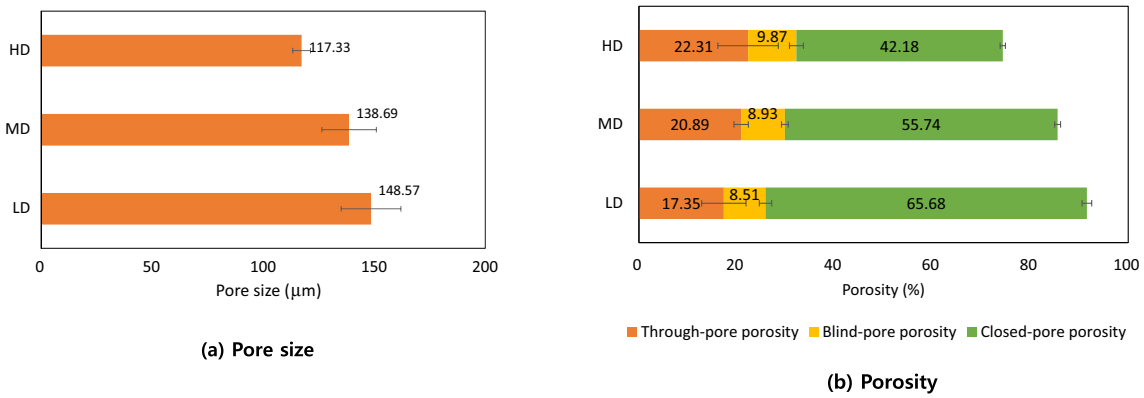

Fig. 3 Results of porosity analysis of balsa depending on density. **a** Pore size, **b** porosity

Eq. 2 was 91.54 ± 1.73^{c} for LD, 85.56 ± 0.14^{b} for MD, and 74.36 ± 0.20^{a}% for HD.

In the porosity analysis, the through-pore porosities of HD and MD were greater than that of LD ($p < 0.01$), and the difference between HD and MD was not statistically significant ($p = 0.433$). However, the closed-pore porosity was in the order of LD > MD > HD ($p < 0.01$).

Table 2 provides results of Pearson's correlation analysis. Total porosity showed a strong positive (+) correlation with closed-pore porosity. However, total porosity showed negative (−) correlations with blind-pore porosity and through-pore porosity.

In solid porous materials, closed-pore porosity is related to thermal conductivity [21, 22], which indicates that the higher is the closed-pore porosity, the greater is the thermal insulation of the porous material. Therefore, to predict the thermal characteristics of the transverse plane of balsa, it is possible to make a prediction based only on total porosity without needing to calculate closed-pore porosity.

Table 2 Results of Pearson's correlation analysis

	Through-pore porosity	Blind-pore porosity	Closed-pore porosity
Total porosity	−0.571**	−0.568**	0.954**

**1% significance level

$n = 39$

The longitudinal permeability of wood is related to properties such as drying, heat transfer, and sound absorption [23–28]. According to our previous studies, gas permeability increases when through-pore porosity is high [17–20]. Therefore, when predicting these properties of balsa, through-pore porosity rather than total porosity should be considered as the main parameter.

Consequently, HD can be more suitable if the balsa transverse plane is to be used as a sound absorbing material. However, if it is to be used as an insulator, LD would be more suitable. These findings need to be confirmed in the future.

Conclusions

1. The porosity of balsa can be classified into through-pore porosity, blind-porosity, and closed-pore porosity.
2. The density of balsa showed the same trend as closed-pore porosity.
3. Through-porosity of HD was the greatest among the three types of balsa.

Abbreviations

LD: Low density; MD: Middle density; HD: High density; D: Pore size (μm); τ: Surface tension of wetting liquid; p: Pressure; C: Constant; ρ: Density of the cylindrical specimen; ρ_{true}: True density of the wood; ϕ_{total}: Total porosity; ϕ_{open}: Open-pore porosity; ϕ_{closed}: Closed-pore porosity; ϕ_{blind}: Blind-pore porosity; $\phi_{through}$: Through-pore porosity; V_{blind}: Blind-pore volume; m_0: Specimen weight; m_1: Specimen weight after Galwick solution extruded; $\rho_{Galwick}$: Density of Galwick solution; V_{total}: Specimen volume.

Acknowledgements

This research was supported by the Basic Science Research Program through the National Research Foundation of Korea (NRF) funded by the Ministry of Education (NRF-2019R1I1A3A02059471) and was supported under the framework of an international cooperation program managed by the NRF of Korea (NRF-2020K2A9A2A08000181). In addition, this research was supported by "Research based construction fund support program" funded by Jeonbuk National University. The authors are also thankful to the "The Business Startup Incubator Support Program" supported by the Ministry of Education and National Research Foundation of Korea. This article is based on the first author (Eun-Suk Jang)'s Jeonbuk National University doctoral thesis.

Author contributions

ESJ: first author, conceptualization, methodology, experiment, data analysis, writing original draft, review, and editing. CWK: corresponding author, supervision and writing review and editing. Both authors read and approved the final manuscript.

Funding

This research was supported by the Basic Science Research Program through the National Research Foundation of Korea (NRF) funded by the Ministry of Education (NRF-2019R1I1A3A02059471) and was supported under the framework of an international cooperation program managed by the NRF of Korea (NRF-2020K2A9A2A08000181).

Availability of data and materials

Not applicable.

Declarations

Competing interests

The authors have no competing interests.

Received: 11 September 2021 Accepted: 6 May 2022
Published online: 26 May 2022

References

1. Kotlarewski NJ, Ozarska B, Gusamo BK (2014) Thermal conductivity of Papua New Guinea balsa wood measured using the needle probe procedure. BioResources 9(4):5784–5793
2. Zhang C, Ma C-Y, Xu L-H, Wu Y-Y, Wen J-l (2021) The effects of mild Lewis acids-catalyzed ethanol pretreatment on the structural variations of lignin and cellulose conversion in balsa wood. Int J Biol Macromol 183(1):1362–1370
3. Borrega M, Gibson LJ (2015) Mechanics of balsa (*Ochroma pyramidale*) wood. Mech Mater 84(1):75–90
4. Shishkina O, Lomov SV, Verpoest I, Gorbatikh L (2014) Structure–property relations for balsa wood as a function of density: modelling approach. Arch Appl Mech 84(6):789–805
5. Da Silva A, Kyriakides S (2007) Compressive response and failure of balsa wood. Int J Solids Struct 44(25–26):8685–8717
6. Easterling K, Harrysson R, Gibson L, Ashby MF (1982) On the mechanics of balsa and other woods. Proceedings of the royal society of London. A. Math Phys Sci 383(1784):31–41
7. Guo G, Finkenstadt VL, Nimmagadda Y (2019) Mechanical properties and water absorption behavior of injection-molded wood fiber/carbon fiber high-density polyethylene hybrid composites. Adv Compos Hybrid Mater 2(4):690–700

8. Jang E-S, Kang C-W, Jang S-S (2018) Comparison of the Mercury Intrusion porosimetry, capillary flow porometry and gas permeability of eleven species of Korean wood. J Korean Wood Sci Technol 46(6):681–691
9. Wheeler E (1989) IAWA list of microscopic features for hardwood identification with an appendix on non-anatomical information. IAWA Bull 10:219–332
10. Borrega M, Ahvenainen P, Serimaa R, Gibson L (2015) Composition and structure of balsa (*Ochroma pyramidale*) wood. Wood Sci Techno 49(2):403–420
11. Pan X, Zhang N, Yuan Y, Shao X, Zhong W, Yang L (2021) Balsa-based porous carbon composite phase change material with photo-thermal conversion performance for thermal energy storage. Sol Energy 230:269–277
12. Rouquerol J, Avnir D, Fairbridge C, Everett D, Haynes J, Pernicone N, Ramsay J, Sing K, Unger K (1994) Recommendations for the characterization of porous solids (technical report). Pure Appl Chem 66(8):1739–1758
13. Dackermann U, Elsener R, Li J, Crews K (2016) A comparative study of using static and ultrasonic material testing methods to determine the anisotropic material properties of wood. Constr Build Mater 102(1):963–976
14. Comstock GL (1970) Directional permeability of softwoods. Wood Fiber Sci 1(4):283–289
15. ASTM F316-03 (2019) Standard test methods for pore size characteristics of membrane filters by bubble point and mean flow pore test. ASTM International, West Conshohocken
16. Smith LM, Shi SQ, Shi J, Wang C, Tan Y, Zhou H (2020) Effect of wood species on the pore volume and surface area of activated carbon derived from the self-activation process. Wood Fiber Sci 52(2):191–207
17. Jang E-S, Yuk J-H, Kang C-W (2020) An experimental study on change of gas permeability depending on pore structures in three species (hinoki, Douglas fir, and hemlock) of softwood. J Wood Sci 66(1):1–12
18. Jang E-S, Kang C-W (2019) Changes in gas permeability and pore structure of wood under heat treating temperature conditions. J Wood Sci 65(1):1–9
19. Jang E-S, Kang C-W (2021) Investigation of sound absorption properties of heat-treated Indonesian Momala (*Homalium foetidum* (Roxb.) Benth.) and Korean red toon (*Toona sinensis* (A. Juss) M. Roem) cross sections. Forests 12(11):1447
20. Jang E-S, Kang C-W (2021) Delignification effects on Indonesian Momala (*Homalium foetidum*) and Korean red toon (*Toona sinensis*) hardwood pore structure and sound absorption capabilities. Materials 14(18):5215
21. Vakifahmetoglu C, Semerci T, Soraru GD (2020) Closed porosity ceramics and glasses. J Am Ceram Soc 103(5):2941–2969
22. Yang S-F, Chiu W-T, Wang T-M, Chen C-T, Tzeng C-C (2014) Porous materials produced from incineration ash using thermal plasma technology. Waste Manage 34(6):1079–1084
23. Taghiyari H, Zolfaghari H, Sadeghi M, Esmailpour A, Jaffari A (2014) Correlation between specific gas permeability and sound absorption coefficient in solid wood. J Trop For Sci 26:92–100
24. Kolya H, Kang C-W (2021) Effective changes in softwood cell walls, gas permeability and sound absorption capability of *Larix kaempferi* (larch) by steam explosion. Wood Mater Sci Eng. https://doi.org/10.1080/17480272.2021.1915864
25. Bao F, Lu J, Avramidis S (1999) On the permeability of main wood species in China. Holzforschung 53(4):350–354
26. Durmaz S, Yildiz UC, Yildiz S (2015) Alkaline enzyme treatment of spruce wood to increase permeability. BioResources 10(3):4403–4410
27. He X, Xiong X, Xie J, Li Y, Wei Y, Quan P, Mou Q, Li X (2017) Effect of microwave pretreatment on permeability and drying properties of wood. BioResources 12(2):3850–3863
28. Li C, Kang C-W, Zhao X-F (2019) Moisture transverse moving mechanism during presteamed oak lumber drying. Sci Rep 9(1):1–6

Publisher's Note